Longitudinal distribution of Na + and Ca 2+ channels and β-adrenoceptors on the sarcolemmal membrane of frog cardiomyocytes

Jonas Jurevičius, Rodolphe Fischmeister

Longitudinal distribution of Na^+ and Ca^{2+} channels and β-adrenoceptors on the sarcolemmal membrane of frog cardiomyocytes

Jonas Jurevičius and Rodolphe Fischmeister*

Laboratoire de Cardiologie Cellulaire et Moléculaire, INSERM U-446, Université de Paris-Sud, Faculté de Pharmacie, F-92296 Châtenay-Malabry, France

1. The distribution of L-type Ca^{2+} and tetrodotoxin-sensitive Na^+ channels and of β-adrenergic receptors was examined in frog ventricular myocytes using the whole-cell patch-clamp technique and a double capillary for extracellular microperfusion.
2. Rod-shaped cells (250–300 μm long) were sealed at both ends to two patch-clamp pipettes and positioned transversally at different positions between the mouths of two micro-capillaries separated by a thin wall. A combination of nifedipine (1 μM) and tetrodotoxin (0·3 μM) (blocking solution) was added to one capillary in order to inhibit macroscopic Ca^{2+} and Na^+ currents (I_{Ca} and I_{Na}, respectively) in the part of the cell exposed to this capillary.
3. Moving the cell in 10–20 μm steps from the control capillary to the capillary containing the blocking solution induced step decreases in I_{Ca} and I_{Na} amplitudes. Complete block of both currents occurred when the entire cell was exposed to the blocking solution.
4. Each step decrease in current was due to the loss of activity of the functional Ca^{2+} and Na^+ channels present in the slice of sarcolemmal membrane newly exposed to the blocking solution. These step current changes allowed longitudinal mapping of current density for Ca^{2+} and Na^+ channels on the sarcolemmal membrane.
5. Addition of a submaximal concentration of isoprenaline (10 nM) to the control capillary induced a local increase in I_{Ca} which enabled examination of the distribution of functional β-adrenergic receptors as well.
6. Our results demonstrate that Ca^{2+} and Na^+ channels and β-adrenergic receptors are equally and essentially uniformly distributed on the sarcolemmal membrane of frog ventricular myocytes.

A number of methods have been developed over the last twenty years to investigate the spatial distribution of ion channels and membrane receptors on the sarcolemmal membranes of various cell types. For instance, autoradiography studies using selective radiolabelled ligands have enabled determination of the distribution of muscarinic (Hartzell, 1980) and β-adrenergic receptors (Molenaar, Canale & Summers, 1987; Wolfe, 1991) in cardiac myocytes. Immunocytochemical methods using either monoclonal antibodies (Westenbroek, Ahlijanian & Catterall, 1990; Carl *et al.* 1995; Carrington, Lynch, Moore, Isenberg, Fogarty & Fay, 1995; Robitaille, Bourque & Vandaele, 1996) or biologically active fluorescent and biotinylated derivatives of a selective ligand (Jones, Kunze & Angelides, 1989) have been used to examine the localization of voltage-dependent Ca^{2+} channels at the neuromuscular junction (Robitaille *et al.* 1996), in neurones (Jones *et al.* 1989; Westenbroek *et al.* 1990) and in smooth (Carrington *et al.* 1995) and cardiac muscle cells (Carl *et al.* 1995). Specific electrophysiological methods have also been designed to examine the distribution of functional, rather than the total number of, ion channels and receptors. For instance, the loose patch-clamp technique was used to study the distribution of Na^+ and K^+ channels in frog skeletal muscle by recording successively the ion currents generated by different areas of one fibre (Almers, Stanfield & Stühmer, 1983). The same technique was combined with UV-light irradiation through the glass micropipette to demonstrate that Na^+ channels do not diffuse readily in the sarcolemma of frog skeletal muscle (Stühmer & Almers, 1982). In the ascidian oocyte, precursor fertilization channels were shown to be uniformly distributed on the surface of the oocyte by comparing the current generated by an entire oocyte in response to a fertilizing spermatozoon with the current generated by small fragments of the oocyte (DeFelice, Dale & Talevi, 1986). Finally, single channel recording from different

regions of neurones (Lipscombe, Madison, Poenie, Reuter, Tsien & Tsien, 1988) or pancreatic β-cells (Bokvist, Eliasson, Ämmälä, Renström & Rorsman, 1995) has demonstrated regional differences in the distribution of Ca^{2+} channels.

In the heart, a number of studies using autoradiographic and immunocytochemical methods have examined the distribution of receptors and channels throughout the heart structure (see e.g. Hartzell, 1980; Molenaar *et al.* 1987; Wolfe, 1991; Carl *et al.* 1995; Gao, Puri, Gerhardstein & Hosey, 1997). However, most of these studies do not provide any information on the functional state of the proteins investigated. The work of Hartzell (1980) is an exception though. In his elegant study, Hartzell demonstrated the random distribution of total as well as functional muscarinic receptors and muscarinic activated K^+ channels in myocytes of the frog sinus venosus by combining (i) autoradiography, to examine the distribution of total QNB (quinuclidinyl benzilate) binding sites, and (ii) electrophysiology, to examine the electrical response of a cardiac fibre to iontophoretic applications of acetylcholine at different places on the sarcolemmal membrane (Hartzell, 1980). However, to our knowledge, there is no available data on the distribution of functional ion channels and receptors at the level of a single isolated cardiac myocyte. One reason for this may be that it is difficult (if not impossible) to record with classic patch-clamp techniques the ion currents from several different and adjacent membrane areas of the same myocyte. Here we took advantage of a recently developed double-barrelled microperfusion technique (Jurevičius & Fischmeister, 1996*a*,*b*) to expose increasing portions of an elongated frog ventricular myocyte to a solution which blocks the activity of Na^+ and L-type Ca^{2+} channels. Step movements of the myocyte from the control solution to the blocking solution allowed a longitudinal mapping of the distribution of Na^+ and Ca^{2+} channels throughout the entire length of the cell.

Preliminary results have appeared in abstract form (Jurevičius & Fischmeister, 1995).

METHODS

Patch-clamp studies with frog ventricular myocytes

Frogs (*Rana esculenta*) were decapitated and double pithed and experiments were performed in accordance with local and national guidelines. Ventricular cells were enzymatically dispersed from the heart with a combination of collagenase (Yakult, Japan) and trypsin (Sigma) as previously described (Fischmeister & Hartzell, 1986). The isolated cells were stored in storage solution (for composition see below) and kept at 4 °C until use (2–48 h after dissociation). Rod-shaped Ca^{2+}-tolerant frog ventricular myocytes (250–400 μm long) were sealed at both ends to two patch-clamp pipettes (1·0–1·5 MΩ) and whole-cell recording conditions were established for both electrodes using two independent patch-clamp amplifiers (RK400; Bio-Logic, Claix, France) as previously described (Jurevičius & Fischmeister, 1996*a*,*b*). One electrode was in voltage-clamp configuration and measured the whole-cell currents while the other was in current-clamp configuration (at zero current) and measured the membrane potential at the most remote part of the cell. Tetrodotoxin-sensitive whole-cell Na^+ current (I_{Na}) was measured by depolarizing the cell every 8 s to −30 mV for 100 ms from a holding potential of −80 mV. After this, the membrane potential returned to −80 mV for 50 ms. The cell was then depolarized to −50 mV for 100 ms to inactivate I_{Na}, and to 0 mV for 200 ms to record the whole-cell L-type Ca^{2+} current (I_{Ca}). K^+ currents were blocked by replacing all K^+ ions with intracellular and extracellular Cs^+ (Fischmeister & Hartzell, 1986). Control solutions (for composition see below) contained 5 nM tetrodotoxin to attenuate the amplitude of I_{Na} and improve voltage control of the myocyte. Under these conditions, the membrane potential measured by the second electrode differed from the command potential by less than 3 mV. I_{Na} and I_{Ca} were measured as the difference between peak inward currents and the currents at the end of the 100 or 200 ms pulse, respectively. All experiments were done at room temperature (19–26 °C).

Microperfusion of single cardiac myocytes

The double-barrelled microperfusion system has been described recently (Jurevičius & Fischmeister, 1996*a*,*b*) and was used here with no modification. After breaking of the patch membrane at the tips of both adjacent electrodes and establishment of whole-cell recording conditions in control Cs–Ringer solution, the cell was positioned transversally at the mouth of the capillary which contained control Cs–Ringer solution (for composition see below) supplemented with 5 nM tetrodotoxin. This was achieved by mounting each electrode holder to the headstage of a three-dimensional vernier-type hydraulic (oil) micromanipulator (OR-60; Narishige, Tokyo, Japan). The control knobs on the remote-control master cylinders had 1 μm graduations for each axis so that movement of the electrodes in each direction was achieved with a precision of ~0·5 μm (half graduation). The headstage of one micromanipulator was mounted on the headstage of the other which allowed simultaneous movement of the adjacent electrodes by rotating the *X*-, *Y*- or *Z*-knobs of just one remote-control stage. Rotating the *X*-knob by ten or twenty graduations moved the cell in 10 or 20 μm steps towards the adjacent capillary so exposing an increasing longitudinal portion of the cell to Cs–Ringer solution supplemented with 300 nM tetrodotoxin and 1 μM nifedipine (blocking solution). Both solutions were flowing out of the capillaries with a linear velocity of ~2 cm s^{-1}.

Solutions and drugs

Storage solution contained (mM): 88·4 NaCl, 2·5 KCl, 23·8 $NaHCO_3$, 0·6 NaH_2PO_4, 1·8 $MgCl_2$, 0·9 $CaCl_2$, 5 creatine, 5 glucose, 5 sodium pyruvate supplemented with 1 μl ml^{-1} non-essential amino acids and vitamin solution, 5000 i.u. ml^{-1} penicillin, 5 mg ml^{-1} streptomycin, adjusted to pH 7·4 with NaOH. Control Cs–Ringer solution contained (mM): 107 NaCl, 10 Hepes, 20 CsCl, 4 $NaHCO_3$, 0·8 NaH_2PO_4, 1·8 $MgCl_2$, 1·8 $CaCl_2$, 5 D-glucose, 5 sodium pyruvate, 5×10^{-6} tetrodotoxin, adjusted to pH 7·4 with NaOH. The 0 Ca Cs–Ringer solution was made by replacing $CaCl_2$ with equimolar $MgCl_2$. Patch-electrodes were filled with control internal solution which contained (mM): 119·8 CsCl, 5 EGTA (acid form), 4 $MgCl_2$, 5 creatine phosphate (disodium salt), 3·1 Na_2ATP, 0·42 Na_2GTP, 0·062 $CaCl_2$ (pCa 8·5), 10 Hepes; adjusted to pH 7·1 with CsOH. Isoprenaline was prepared as a stock solution of 1 mM in 5 mM ascorbic acid. Each day a fresh 10 mM stock solution of nifedipine was prepared in ethanol and stored at 4 °C. Immediately before being applied onto the cell, nifedipine was dissolved to give the desired final concentration. Care was taken to protect nifedipine against irradiation from natural light. Tetrodotoxin was from Latoxan (Rosans, France) and all other drugs were from Sigma.

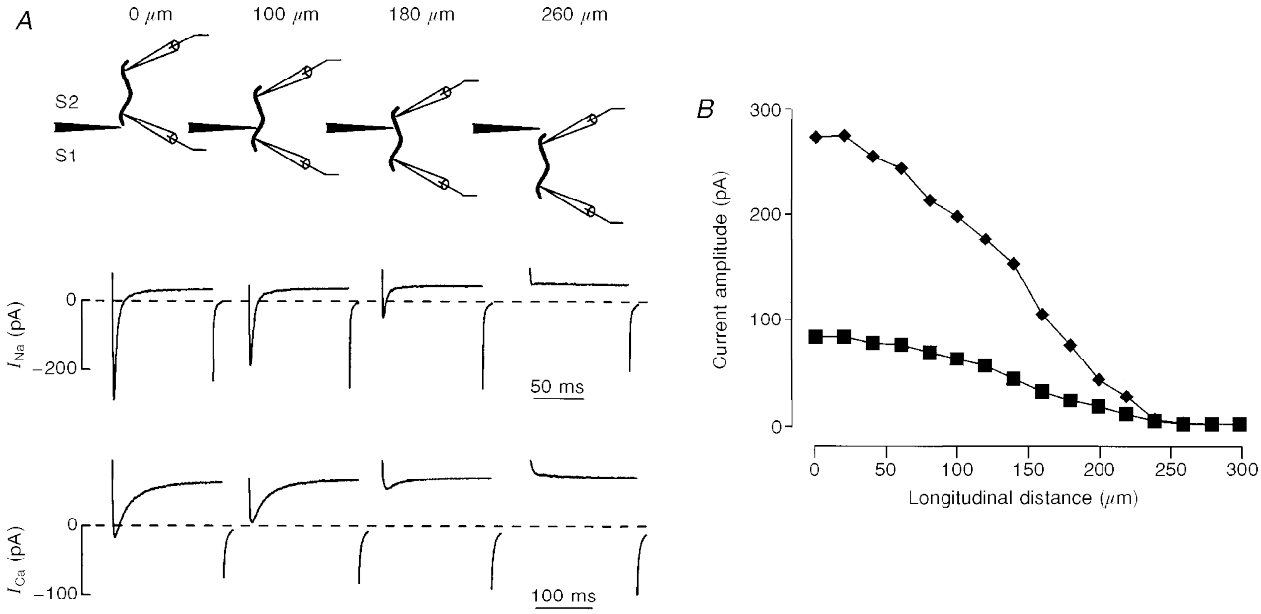

Figure 1. Longitudinal spatial profiles of Na^+ and L-type Ca^{2+} channels in a frog ventricular myocyte

A, top, as indicated by the leftmost drawing, the cell was initially exposed to solution S2, in this case Cs–Ringer solution supplemented with 5 nM tetrodotoxin. The corresponding I_{Na} and I_{Ca} current traces are shown below. The cell was then progressively immersed in 20 μm longitudinal step movements in S1 blocking solution composed of Cs–Ringer supplemented with 300 nM tetrodotoxin and 1 μM nifedipine. The I_{Na} and I_{Ca} current traces corresponding to two intermediate positions (100 μm and 180 μm) are shown. Finally, at position 260 μm, the cell was totally exposed to S1, and the current traces show a complete blockade of I_{Na} and I_{Ca}. *B*, variation in amplitude of I_{Na} (◆) and I_{Ca} (■) as a function of the longitudinal position of the cell with respect to the S1 capillary.

RESULTS

The double-barrelled microperfusion system described previously (Jurevičius & Fischmeister, 1996*a*,*b*) was used to expose a frog ventricular myocyte to one of two extracellular solutions (S1 or S2) flowing out of two adjacent microcapillaries. At intermediate positions between the two capillaries, it was possible to expose one portion of the cell to S1 while the rest of the cell was superfused by S2. The diagram at the top of Fig. 1*A* illustrates how the experiments were performed. In this experiment, S2 was composed of Cs–Ringer solution supplemented with 5 nM tetrodotoxin to reduce I_{Na}. S1 contained a higher concentration of tetrodotoxin (300 nM) and 1 μM nifedipine (blocking solution) to completely block I_{Na} and I_{Ca}, respectively. When the cell was entirely exposed to S2 (Fig. 1*A*, at 0 μm), control I_{Na} and I_{Ca} were recorded. As the cell was progressively immersed in S1, both currents decreased as shown by the individual current traces at the two intermediate positions (Fig. 1*A*, 100 and 180 μm). When the entire cell was exposed to S1, I_{Na} and I_{Ca} were fully blocked (Fig. 1*A*, position 260 μm). Figure 1*B* shows the variation in amplitude of I_{Na} and I_{Ca} obtained during 20 μm successive steps from S2 to S1. As shown, both current amplitudes

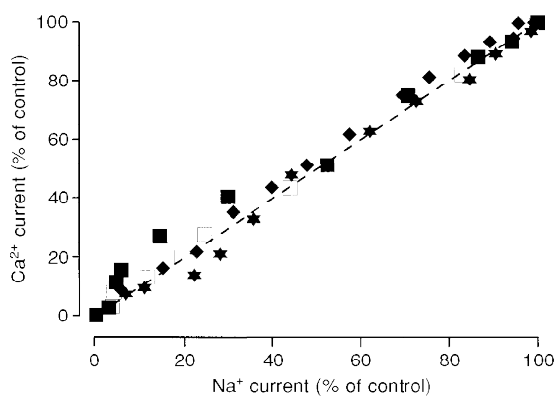

Figure 2. Equal longitudinal distribution of Na^+ and Ca^{2+} channels in frog ventricular myocytes

Each symbol corresponds to a different cell under the same protocol as in Fig. 1. I_{Na} and I_{Ca} amplitudes were normalized with respect to their maximal amplitude (100%) measured when the cell was entirely exposed to S2, i.e. to Cs–Ringer solution supplemented with 5 nM tetrodotoxin. The data points were fitted to the linear function $y = ax + b$ using least-squares regression analysis. The result of the fit is indicated by the dashed line, which corresponds to a (slope) and b (intercept) values of 0·99 and 1·3% ($r = 0·99$), respectively.

decreased as a sigmoidal function of the distance of immersion of the cell in the blocking solution. When normalized to the control amplitude measured in S2, both currents decreased with a similar relationship. This is illustrated in more detail in Fig. 2 where the results from four experiments (different symbol for each) similar to that shown in Fig. 1 are pooled and the normalized I_{Ca} amplitude is plotted as a function of the normalized I_{Na} amplitude, the data points are positioned along a straight line of slope 1 (dashed line). This demonstrates that, on a 20 μm scale in the longitudinal direction of the cell, functional Na^+ and L-type Ca^{2+} channels are equally distributed on the sarcolemmal membrane.

The activity of L-type Ca^{2+} channels is strongly stimulated by activation of β-adrenergic receptors (McDonald, Pelzer, Trautwein & Pelzer, 1994). However, the distribution of functional β-adrenergic receptors on the sarcolemmal membrane is unknown. Since we have shown recently, using the microperfusion technique, that β-adrenergic receptors are essentially coupled to nearby Ca^{2+} channels in frog ventricular myocytes (Jurevičius & Fischmeister, 1996*a*), it is possible to determine the distribution of functional β-adrenergic receptors by comparing the distribution of isoprenaline-stimulated Ca^{2+} channels with that of basal Ca^{2+} channels. Figure 3 shows such an experiment. In this experiment the cell was moved in 10 μm steps from S2 (control Cs–Ringer) to S1 (0 Ca Cs–Ringer solution), this was then repeated twice more with capillary solutions supplemented with 10 nM and 1 μM isoprenaline. In the absence of isoprenaline when the cell was entirely immersed in S2 control I_{Ca} was ~70 pA. The current progressively decreased to 0 pA as the cell moved towards total immersion in S1. After the distribution of basal I_{Ca} was obtained (Fig. 3*A*, circles), the cell was returned to total immersion in S2 and both S1 and S2 were supplemented with 10 nM isoprenaline. This small concentration of isoprenaline increased I_{Ca} to ~200 pA while the cell was in S2. The cell was again moved from S2 to S1 in 10 μm steps and the distribution of stimulated I_{Ca} was obtained (Fig. 3*A*, open squares). Finally, the cell was returned to S2 and 1 μM isoprenaline was added to both solutions. This induced a maximal increase in I_{Ca}, to an amplitude of ~800 pA while the cell was in S2. Moving the cell again stepwise from S2 to S1 revealed the distribution of I_{Ca} maximally stimulated by isoprenaline (Fig. 3*A*, filled squares). All three curves obtained (Fig. 3*A*) had a similar sigmoidal shape. Figure 3*B* presents the data from Fig. 3*A* differently. At each position on the longitudinal axis between S2 and S1, three I_{Ca} amplitudes were obtained: basal I_{Ca} ($I_{Ca,0}$), isoprenaline (10 nM)-stimulated I_{Ca} ($I_{Ca,1}$) and isoprenaline (1 μM)-stimulated I_{Ca} ($I_{Ca,2}$). The differences, $I_{Ca,1} - I_{Ca,0}$ (open squares) and $I_{Ca,2} - I_{Ca,0}$ (filled squares), are plotted as a function of $I_{Ca,0}$. These differences indicate the amount of

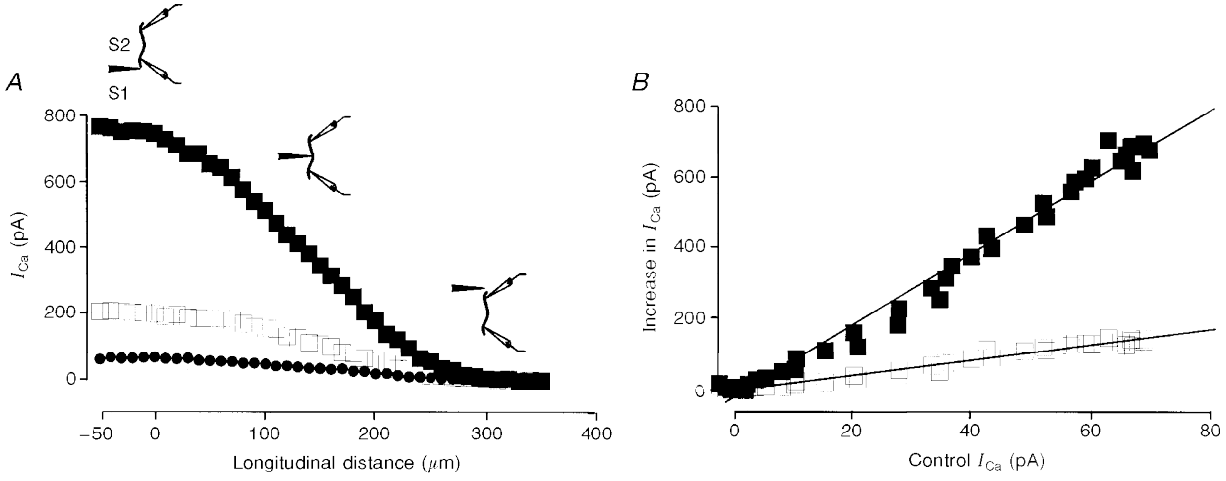

Figure 3. Equal longitudinal distribution of Ca^{2+} channels and β-adrenergic receptors in frog ventricular myocytes

Variation in amplitude of I_{Ca} as a function of the longitudinal position of the cell with respect to S1. For control conditions (●), S1 and S2 were the same as in Fig. 1. □, both solutions were supplemented with 10 nM isoprenaline. ■, the concentration of isoprenaline was increased to 1 μM in both solutions. For all conditions, the cell was first exposed to S2 then moved in 10 μm longitudinal steps towards S1, as indicated by the illustrations above the curve. Position 0 μm corresponded to the last position in S2 before the amplitude of I_{Ca} started to decrease. After thirty step movements, i.e. at position 300 μm, I_{Ca} was fully blocked, i.e. the cell was totally immersed in S1. Further movements had no additional effect on the currents. *B*, for each longitudinal position, variation in I_{Ca} amplitude in response to 10 nM (□) or 1 μM (■) isoprenaline was plotted as a function of the amplitude of control I_{Ca}, i.e. in the absence of isoprenaline. Data points were fitted to linear functions $y = ax + b$ using least-squares regression analysis. The results of the fits are shown as two continuous lines, with a (slope) and b (intercept) values of, respectively, 1·04 and −0·01 pA ($r = 0{\cdot}99$) for 10 nM isoprenaline, and 1·02 and −1·46 pA ($r = 0{\cdot}99$) for 1 μM isoprenaline.

additional I_{Ca} originating from submaximal or maximal activation of β-adrenergic receptors. As shown in Fig. 3*B*, both relationships were linear. The experiment shown in Fig. 3 is representative of four similar experiments. Thus, on a 10 μm scale in the longitudinal direction of the cell, functional β-adrenergic receptors and L-type Ca^{2+} channels are equally distributed on the sarcolemmal membrane.

Our results so far demonstrate that functional Na^+ channels, L-type Ca^{2+} channels and β-adrenergic receptors present a similar membrane distribution along the longitudinal axis of a frog ventricular myocyte. Such a similarity in the distribution of these three quite different membrane proteins may indicate that all three proteins are randomly distributed in the sarcolemmal membrane. Confirmation of a random distribution would require that each variation in I_{Na} or in basal or isoprenaline-stimulated I_{Ca} observed when moving the cell from one capillary to the other be associated with an independent measurement of the increment of membrane area immersed in the new solution. Unfortunately, this was not technically feasible in our experiments. However, microscopic evaluation of the myocyte indicated a spindle-like morphology as already described by others (Hume & Giles, 1981; Arrio-Dupont & De Nay, 1985). Thus, the simplest and most extreme representation of the 3D geometry of the myocyte is that of a perfect cylinder. Figure 4 shows what can be inferred from such a hypothesis. In this experiment, the longitudinal distribution of isoprenaline (1 μM)-stimulated I_{Ca} was examined, as in Fig. 3*A*. The upper panel shows thirty-two individual I_{Ca} traces obtained during thirty-two successive 10 μm step movements from S1 (0 Ca Cs–Ringer) to S2 (Cs–Ringer), both supplemented with 1 μM isoprenaline, over a total distance of 320 μm. I_{Ca} increased from 0 pA to

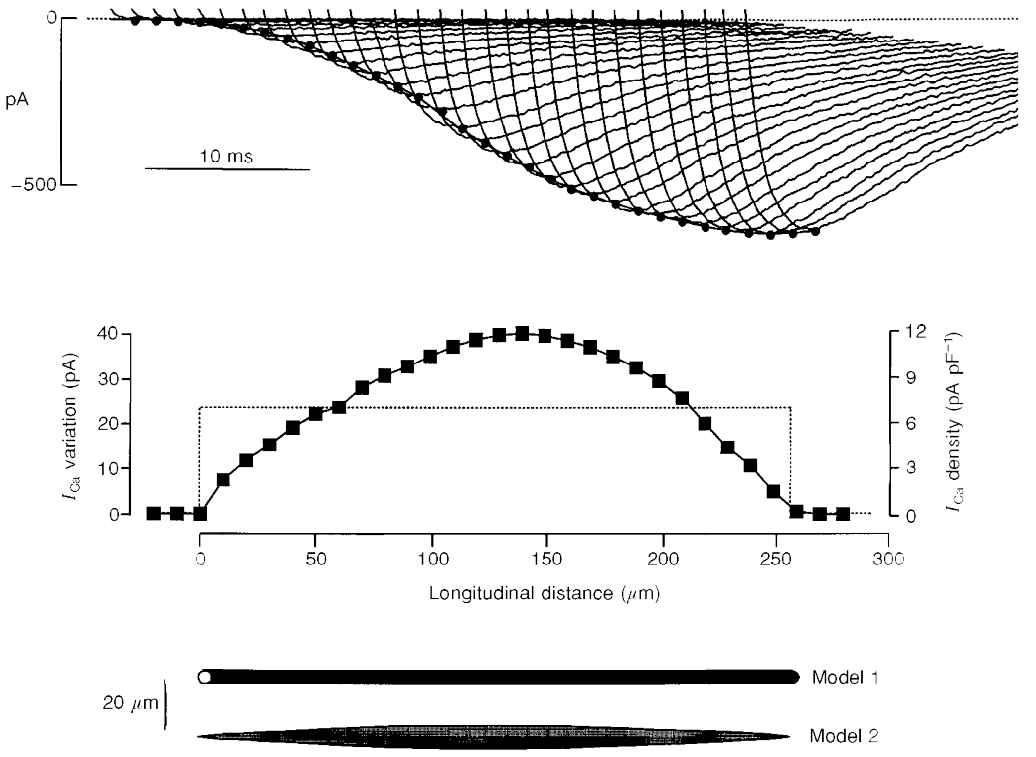

Figure 4. Two possible interpretations of the longitudinal distribution of Ca^{2+} channels in a frog ventricular myocyte

The upper panel shows the beginning of thirty-two individual I_{Ca} traces, obtained in a frog ventricular myocyte at 0 mV membrane potential during thirty-two successive 10 μm step movements from a 0 Ca Cs–Ringer solution (S1) to Cs–Ringer solution (S2), both solutions supplemented with 1 μM isoprenaline. The cell was moved within 1 s during the 8 s interval that separated two consecutive depolarizations, and over a total distance of 320 μm. For clarity, each current trace is shifted to the right by ~1·3 ms with respect to the preceding trace. For each trace, ● indicates the position of peak current amplitude. In the middle panel squares represent the I_{Ca} increments (in pA, left scale) between two consecutive movements and are plotted as a function of the length of the cell immersed in S2. The cell had a membrane capacitance of 88 pF. If one assumes that the cell is cylindrical (Model 1 in the bottom panel, drawn to scale), then the data points can be converted to I_{Ca} density increments (in pA pF^{-1}, right scale in the middle panel) revealing a bell-shaped distribution of Ca^{2+} channels in the longitudinal direction of the cell. However, if one assumes that the density of functional Ca^{2+} channels is uniform throughout the length of the cell, then the mean I_{Ca} density is estimated to be 7·1 pA pF^{-1} (dotted line in the middle panel) and the geometry of the cell thought to be that of Model 2 (bottom panel). (For further details, see text.)

a maximal amplitude ($I_{Ca,max}$) of 625 pA. The data points in the middle panel of Fig. 4 (squares) show the current increments (in pA, left scale) between two consecutive movements. Total length of the cell (l) can be estimated by the number of 10 μm segments that separate the first and the last series of zero current increments, i.e. $l = 260$ μm. Since the whole-cell membrane capacitance (C_m) was 88 pF in this experiment, and frog cardiac myocytes have a specific cell membrane capacitance of $\sim$2·2 μF cm^{-2} (Hume & Giles, 1981), the cell membrane surface area (S) was calculated to be $\sim$4000 μm^2 and the cell diameter was $S/\pi l = 4{\cdot}9$ μm (Fig. 4, Model 1). Thus, each 10 μm segment of the cell would correspond to a portion of membrane equal to $S/26 = 154$ μm^2 and a membrane capacitance of $C_m/26 = 3{\cdot}4$ pF. Current density values (in pA pF^{-1}, Fig. 4, middle panel, right scale) can be derived from the current increment data. Such an analysis reveals a bell-shaped distribution of Ca^{2+} channels in the longitudinal direction of the cell. Thus, if the geometry of the cell is that of Model 1 (Fig. 4), the distribution is not uniform but, on the contrary, each extremity of the cell has a rather small Ca^{2+} channel density, and this density progressively increases towards a maximum of $\sim$11 pA pF^{-1} when approaching the centre of the cell. Another extreme hypothesis is to assume that the distribution of functional Ca^{2+} channels is random, i.e. is perfectly uniform throughout the length of the cell. In such a case, the mean i_{ca} density would be $I_{Ca,max}/C_m$, i.e. 7·1 pA pF^{-1} (dotted line in Fig. 4). Under such a hypothesis, each current increment would be proportional to the surface of membrane present in the 10 μm segment of the cell. This would imply that the geometry of the cell is that of Model 2 (Fig. 4). According to this second hypothesis, the cell would have thin extremities, and its diameter would increase progressively towards a maximum of 7·7 μm around the centre of the cell, perhaps where the nucleus is located.

DISCUSSION

Our study demonstrates that functional Na^+ channels, L-type Ca^{2+} channels and β-adrenergic receptors present a similar membrane distribution along the longitudinal axis of a frog ventricular myocyte. The simplest explanation of these findings is that these three proteins are actually randomly distributed in the sarcolemmal membrane. A uniform distribution of Na^+ and L-type Ca^{2+} channels would contribute to the homogenous propagation of electrical activity and, together with a random distribution of β-adrenergic receptors, to a synchronized generation and development of sarcomere shortening during the basal or stimulated mechanical activity of the cell. This may be of particular importance in the amphibian and embryonic mammalian hearts in which the sarcoplasmic reticulum (SR) is less developed than in adult mammalian hearts, and propagation of Ca^{2+} released from SR may be low (see e.g. Morad & Cleeman, 1987). A uniform distribution would also imply that the geometry of the frog cardiac myocyte be roughly that of Model 2 in Fig. 4, which is compatible with earlier data showing that frog cardiac myocytes are thicker in their middle panel, around the nucleus, than in the rest of the cell (see e.g. Hume & Giles, 1981; Arrio-Dupont & De Nay, 1985). Finally, a uniform distribution of functional Na^+ channels, L-type Ca^{2+} channels and β-adrenergic receptors would be consistent with the findings that two other membrane proteins, the muscarinic receptors and the muscarinic activated K^+ channels, are also randomly distributed in frog cardiac myocytes (Hartzell, 1980).

A major advantage of our experimental approach is that it allows us to examine the distribution of functional proteins rather than the distribution of the total number of proteins as visualized by autoradiography or immunocytochemistry. This may be particularly relevant to L-type Ca^{2+} channels since the number of functional channels may be much smaller than the total number of dihydropyridine receptors (Aiba & Creazzo, 1993; but see Lew, Hryshko & Bers, 1991). However, one limitation of our approach is its space resolution. The three proteins investigated here can be assumed to be uniformly distributed only on a 10 μm length scale and in the longitudinal direction. Indeed, the signal-to-noise ratio was not sufficient to estimate current variations corresponding to step movements of less than 10 μm. Thus, we cannot exclude the possibility that, within this 10 μm length, Na^+ channels, L-type Ca^{2+} channels and β-adrenergic receptors are located in clusters. This was actually found to be the case for Na^+ and K^+ channels at the frog neuromuscular junction (Almers *et al.* 1983), and for L-type Ca^{2+} channels in neurones (Westenbroek *et al.* 1990). In rabbit ventricular myocytes, immunolocalization techniques have demonstrated that L-type Ca^{2+} channels are located almost exclusively in the transverse (T-) tubules, which are spaced at approximately 2 μm intervals along the whole length of the cell (Carl *et al.* 1995; Gao *et al.* 1997). A clustering behaviour of L-type Ca^{2+} channels has also been demonstrated in chick embryonic cardiac myocytes using the cell-attached patch-clamp technique (e.g. DeFelice, 1993).

Aiba, S. & Creazzo, T. L. (1993). Comparison of the number of dihydropyridine receptors with the number of functional L-type calcium channels in embryonic heart. *Circulation Research* **72**, 396–402.

Almers, W., Stanfield, P. R. & Stühmer, W. (1983). Lateral distribution of sodium and potassium channels in frog skeletal muscle: measurements with a patch-clamp technique. *Journal of Physiology* **336**, 261–284.

Arrio-Dupont, M. &. De Nay, D. (1985). High yield preparation of calcium-tolerant myocytes from frog ventricles. Some properties of the isolated cells. *Biology of the Cell* **54**, 163–170.

Bokvist, K., Eliasson, L., Ämmälä, C., Renström, E. & Rorsman, P. (1995). Co-localization of L-type Ca^{2+} channels and insulin-containing secretory granules and its significance for the initiation of exocytosis in mouse pancreatic β-cells. *EMBO Journal* **14**, 50–57.

Carl, S. L., Felix, K., Caswell, A. H., Brandt, N. R., Ball, W. J., Vaghy, P. L., Meissner, G. & Ferguson, D. G. (1995). Immunolocalization of sarcolemmal dihydropyridine receptor and sarcoplasmic reticular triadin and ryanodine receptor in rabbit ventricle and atrium. *Journal of Cell Biology* **129**, 673–682.

Carrington, W. A., Lynch, R. M., Moore, E. D. W., Isenberg, G., Fogarty, K. E. & Fay, F. S. (1995). Superresolution three-dimensional images of fluorescence in cells with minimal light exposure. *Science* **268**, 1483–1487.

DeFelice, L. J. (1993) Molecular and biophysical view of the Ca channel: A hypothesis regarding oligomeric structure, channel clustering, and macroscopic current. *Journal of Membrane Biology* **133**, 191–202.

DeFelice, L. J., Dale, B. & Talevi, R. (1986). Distribution of fertilization channels in ascidian oocyte membranes. *Proceedings of the Royal Society* B **229**, 209–214.

Fischmeister, R. & Hartzell, H. C. (1986). Mechanism of action of acetylcholine on calcium current in single cells from frog ventricle. *Journal of Physiology* **376**, 183–202.

Gao, T., Puri, T., Gerhardstein, B. & Hosey, M. (1997). Expression, localization and association of L-type Ca channel subunits in cardiac myocytes. *Biophysical Journal* **72**, A147.

Hartzell, H. C. (1980). Distribution of muscarinic acetylcholine receptors and presynaptic nerve terminals in amphibian heart. *Journal of Cell Biology* **86**, 6–20.

Hume, J. R. & Giles, W. (1981). Active and passive electrical properties of single bullfrog atrial cells. *Journal of General Physiology* **78**, 19–42.

Jones, O. T., Kunze, D. L. & Angelides, K. J. (1989). Localization and mobility of omega-conotoxin sensitive Ca^{2+} channels in hippocampal Ca1 neurons. *Science* **244**, 1189–1193.

Jurevičius, J. & Fischmeister, R. (1995). Uniform distribution of Na^{+} and Ca^{2+} channels in the sarcolemma of frog cardiac myocytes *Journal of Molecular and Cellular Cardiology* **27**, A128.

Jurevičius, J. & Fischmeister, R. (1996*a*). cAMP compartmentation is responsible for a local activation of cardiac Ca^{2+} channels by β-adrenergic agonists. *Proceedings of the National Academy of Sciences of the USA* **93**, 295–299.

Jurevičius, J. & Fischmeister, R. (1996*b*). Acetylcholine inhibits Ca^{2+} current by acting exclusively at a site proximal to adenylyl cyclase in frog cardiac myocytes. *Journal of Physiology* **491**, 669–675.

Lew, W. Y. W., Hryshko, L. V. & Bers, D. M. (1991). Dihydropyridine receptors are primarily functional L-type calcium channels in rabbit ventricular myocytes. *Circulation Research* **69**, 1139–1145.

Lipscombe, D., Madison, D. V., Poenie, M., Reuter, H., Tsien, R. Y. & Tsien, R. W. (1988).. Spatial distribution of calcium channels and cytosolic calcium transients in growth cones and cell bodies of sympathetic neurons. *Proceedings of the National Academy of Sciences of the USA* **85**, 2398–2402.

McDonald, T. F., Pelzer, S., Trautwein, W. & Pelzer, D. J. (1994). Regulation and modulation of calcium channels in cardiac, skeletal, and smooth muscle cells. *Physiological Reviews* **74**, 365–507.

Molenaar, P., Canale, E. & Summers, R. J. (1987). Autoradiographic localization of beta-1 and beta-2 adrenoceptors in guinea pig atrium and regions of the conducting system. *Journal of Pharmacology and Experimental Therapeutics* **241**, 1048–1064.

Morad, M. & Cleemann, L. (1987). Role of Ca^{2+} channel in development of tension in heart muscle. *Journal of Molecular and Cellular Cardiology* **19**, 527–553.

Robitaille, R., Bourque, M. J. & Vandaele, S. (1996). Localization of L-type Ca^{2+} channels at perisynaptic glial cells of the frog neuromuscular junction. *Journal of Neuroscience* **16**, 148–158.

Stühmer, W. & Almers, W. (1982). Photobleaching through glass micropipettes: Sodium channels without lateral mobility in the sarcolemma of frog skeletal muscle. *Proceedings of the National Academy of Sciences of the USA* **79**, 946–950.

Westenbroek, R. E., Ahlijanian, M. K. & Catterall, W. A. (1990). Clustering of L-Type Ca^{2+} channels at the base of major dendrites in hippocampal pyramidal neurons. *Nature* **347**, 281–284.

Westenbroek, R. E., Sakurai, T., Elliott, E. M., Hell, J. W., Starr, T. V. B., Snutch, T. P. & Catterall, W. A. (1995). Immunochemical identification and subcellular distribution of the α1A subunits of brain calcium channels. *Journal of Neuroscience* **15**, 6403–6418.

Wolfe, B. B. (1991). Autoradiographic studies of beta-adrenergic receptors. In *The β-Adrenergic Receptors*, ed. Perkins, J. P., pp. 263–293. The Humana Press Inc., Totowa, NJ, USA.

Acknowledgements

We thank Patrick Lechêne for skilful technical assistance, F. Lefebvre and I. Ribaud for preparation of the cells, and Drs P.-F. Méry, V. Veksler and A. V. Skeberdis for helpful discussions. This work was supported by a grant from the Fondation pour la Recherche Médicale.

Author's permanent address

J. Jurevičius: Kaunas Medical Academy, Institute of Cardiology, Laboratory of Membrane Biophysics, Kaunas3007, Lithuania.

Author's email address

R. Fischmeister: Fisch@vjf.inserm.fr